Bioinorganic Chemistry

DOI: 10.1002/anie.201208044

A Tetracarbene–Oxoiron(IV) Complex**

*Steffen Meyer, Iris Klawitter, Serhiy Demeshko, Eckhard Bill, and Franc Meyer**

Dedicated to Professor Karl Wieghardt on the occasion of his 70th birthday

Oxoiron(IV) species are key intermediates in the catalytic cycles of numerous heme and non-heme iron enzymes that insert an oxygen atom from dioxygen into unactivated C–H bonds.[1] Because of the enormous importance of such oxygenase reactions in biology and in synthetic chemistry, much effort has been devoted over the last decade to the isolation and characterization of those reactive oxoiron(IV) intermediates and to the understanding of their reactivity patterns.[2–4] Following the first evidence for the generation of a non-heme Fe^{IV}=O complex in 2000,[5] six X-ray crystallographic structures of oxoiron(IV) complexes have meanwhile been reported;[6–11] all are based on tetra- or pentadentate N-donor ligands, such as derivatives of 1,4,8,11-tetraazacyclotetradecane (cyclam)[6,8] or tris(aminoethyl)amine (tren).[9,10]

Similar N-donor ligands have also been used in related iron–nitrido chemistry,[12,13] though N-heterocyclic carbene (NHC) ligands, mostly tridentate ones with threefold symmetry, have proven particularly useful to stabilize and isolate high-valent Fe≡N species.[14,15] Cramer and Jenkins recently developed a macrocyclic tetracarbene–iron catalyst for the aziridination of alkenes with aryl azides; mass spectrometry confirmed an iron(IV) imide as potential intermediate.[16] Here, we report the efficient stabilization of the oxoiron(IV) unit by such a macrocyclic tetracarbene framework,[17] thus allowing the first structural characterization of an oxoiron(IV) complex that is not purely N ligated and has spectroscopic signatures distinct from those of other oxoiron(IV) complexes.

Tetracarbene–iron(II) precursor complex **1** was generated by in situ deprotonation and complexation of the macrocyclic tetraimidazolium salt $[(L^{NHC})H_4](OTf)_4$ (3,9,14,20-tetraaza-1,6,12,17-tetraazoniapenta-cyclohexacosane-1(23),4,6(26),10,12(25),15,17(24),21-octaene tetrakis-trifluoromethanesulfonate)[18] with $[Fe\{N(SiMe_3)_2\}_2]_2$ in around 30% yield, similar to the synthesis of its phenyl-substituted derivative (Scheme 1).[16,19] While ESI-MS shows $[(L^{NHC})Fe(OTf)_2]^+$ ($m/z = 702.0$, calcd $m/z = 702.0$) and its fragments, X-ray diffraction reveals that, instead of the anionic triflate counter-

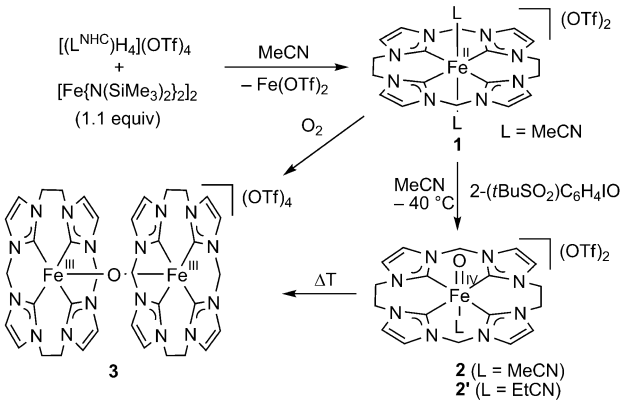

Scheme 1. Synthetic routes to $[(L^{NHC})Fe(MeCN)_2](OTf)_2$ (**1**), $[(L^{NHC})Fe^{IV}O(RCN)](OTf)_2$ (**2**/**2'**), and $[(L^{NHC})_2Fe_2O](OTf)_4$ (**3**).

anions, MeCN molecules are coordinated as axial ligands to give an octahedral environment for **1** in solid state (Figure 1, left). The well-resolved NMR spectrum of **1** indicates low-spin iron(II), and the Mössbauer isomer shift ($\delta = 0.23\ mm\,s^{-1}$; Figure S1, see the Supporting Information) is in agreement with that of another octahedral low-spin tetracarbene–iron(II) complex ($\delta = 0.15\ mm\,s^{-1}$).[20] The large quadrupole splitting for **1** ($\Delta E_Q = 2.10\ mm\,s^{-1}$) is unusual for the formally symmetric $3d^6$ low-spin configuration, but not unprecedented for complexes with strongly asymmetric

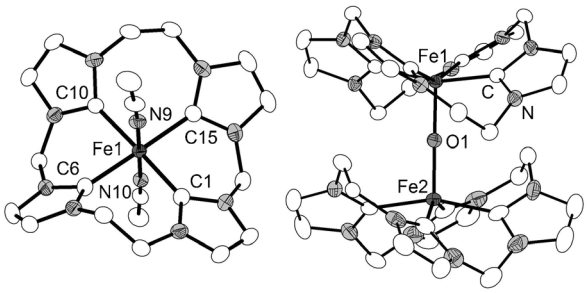

Figure 1. ORTEP plots of the molecular structures of the cations of $[(L^{NHC})Fe(MeCN)_2](OTf)_2$ (**1**, left) and $[(L^{NHC})_2Fe_2O](OTf)_4$ (**3**, right). **1**: 50% probability thermal ellipsoids; co-crystallized $[Fe(MeCN)_4(OTf)_2]$, counter ions, and solvent molecules were omitted for clarity; **3**: 30% probability thermal ellipsoids; counter ions and solvent molecules were omitted for clarity.

[*] S. Meyer, I. Klawitter, Dr. S. Demeshko, Prof. Dr. F. Meyer
Institut für Anorganische Chemie
Georg-August Universität Göttingen
Tammannstr. 4, 37077 Göttingen (Germany)
E-mail: franc.meyer@chemie.uni-goettingen.de
Homepage: http://www.meyer.chemie.uni-goettingen.de
Dr. E. Bill
Max-Planck-Institut für chemische Energiekonversion
Stiftstrasse 34–36, 45470 Mülheim an der Ruhr (Germany)

[**] Financial support from the DFG (International Research Training Group GRK 1422 "Metal Sites in Biomolecules: Structures, Regulation and Mechanisms"; see http://www.biometals.eu) is gratefully acknowledged.

Supporting information for this article is available on the WWW under http://dx.doi.org/10.1002/anie.201208044.

covalent bonds.[21–23] Complex **1** is moisture and oxygen sensitive and well soluble in polar solvents.

Treatment of **1** with an excess of a PhIO derivative, namely 2-(*tert*-butylsulfonyl)iodosylbenzene (2-(tBuSO$_2$)-C$_6$H$_4$IO), in MeCN at −40 °C gives a green suspension, from which excess of insoluble 2-(tBuSO$_2$)C$_6$H$_4$IO was removed by decantation. ESI-MS of the resulting green solution showed two dominant signals for $[(L^{NHC})FeO(OTf)]^+$ (m/z = 569.0, calcd m/z = 569.1) and $[(L^{NHC})FeO]^{2+}$ (m/z = 210.0, calcd m/z = 210.1; Figure 2), which confirmed the formation of oxoiron(IV) complex **2** (Scheme 1).

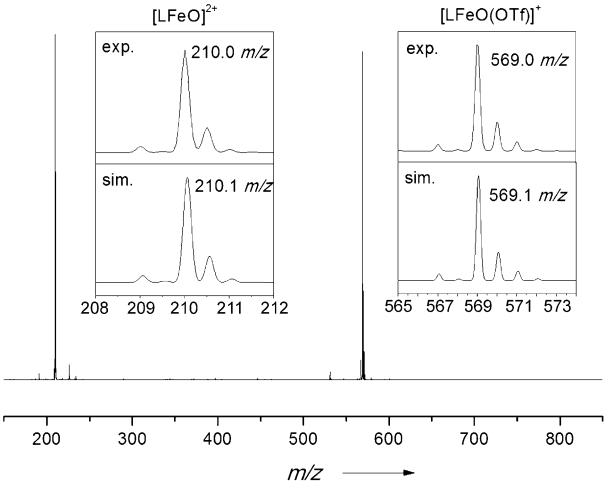

Figure 2. ESI$^+$-MS spectrum (m/z = 250–850 range) of $[(L^{NHC})Fe^{IV}O(MeCN)](OTf)_2$ in MeCN. Insets show experimentally obtained (exp.) and simulated (sim.) isotope patterns.

The transfer of the oxygen atom was monitored by UV/Vis spectroscopy at −40 °C, showing a decrease of the band at 339 nm (characteristic for **1**, $\varepsilon = 9100\,M^{-1}cm^{-1}$), while a much broader band concurrently arises at around 400 nm (characteristic for **2**, $\varepsilon \approx 200\,M^{-1}cm^{-1}$; Figure 3). Typically, oxoiron(IV) chromophores show very weak transitions in the near-IR 700–900 nm region.[4] Time traces of the bands at 339 and 400 nm suggest a more complex reaction sequence; identification of intermediates and detailed kinetic studies are ongoing. Full conversion to **2** was achieved after approximately two hours.

Green single crystals of the oxoiron(IV) complex **2′** suitable for X-ray diffraction were obtained by slow diffusion of Et$_2$O into a EtCN solution at −40 °C. Complex **2′** crystallizes in the orthorhombic space group *Pbca*. The molecular structure shows planar fourfold carbene coordination, and the oxygen atom as well as an EtCN solvent molecule as *trans* axial ligands (Figure 4, left). The Fe–O bond length is 1.661(3) Å, which is at the upper end of the range of the three previously structurally characterized intermediate-spin (S = 1) Fe^{IV}=O complexes (1.639–1.667 Å),[6,7,8] while two reported high-spin (S = 2) Fe^{IV}=O complexes form similar or slightly longer bonds (1.661 and 1.680 Å).[9,10] It should be kept in mind, though, that in contrast to **2′**, all literature-known Fe^{IV}=O complexes are

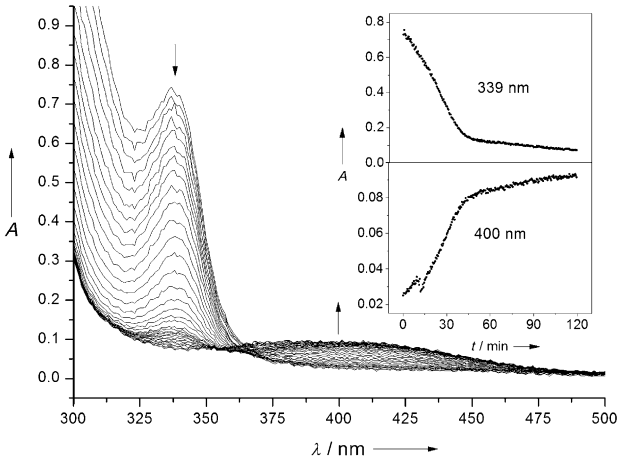

Figure 3. Formation of $[(L^{NHC})Fe^{IV}O(MeCN)](OTf)_2$ (**2**) from **1** after addition of five equivalents of 2-(tBuSO$_2$)C$_6$H$_4$IO in CH$_2$Cl$_2$ to a solution of **1** in MeCN at −40 °C, as monitored by UV/Vis spectroscopy. The insets show the development of bands at 339 and 400 nm versus time.

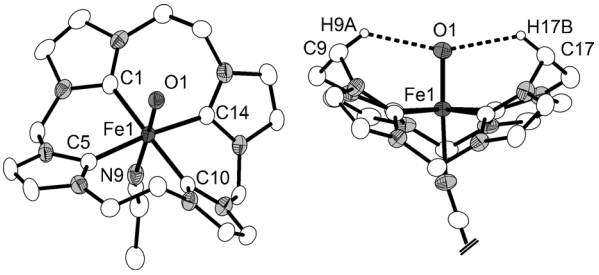

Figure 4. Two views (ORTEP plots, 50% probability thermal ellipsoids) of the molecular structures of $[(L^{NHC})Fe^{IV}O(EtCN)](OTf)_2$ (**2′**); counter ions and solvent molecules omitted for clarity. The structure on the right emphasizes the intramolecular C-H···O hydrogen bonds (Et group of the EtCN not shown). Selected atom distances [Å] and angles [°]: O1···H9A = 2.31, O1···H17B = 2.35, O1···C9 = 3.036(6), O1···C17 = 3.078(6); C9-H9A···O1 = 130.5, C17-H17B···O1 = 131.6.

exclusively N/O-coordinated. Fe–C distances in **2′** vary between 1.979(5) and 2.045(5) Å, with short and long bond lengths *trans* to each other (Table 1). The N–Fe–O bond angle is 176.65(17)° and *trans* C–Fe–C angles are 174.00(19)° and 172.92(19)°, thus forming a nearly perfect octahedral coordination geometry. It is interesting to note that one carbon atom of each ethylene bridge of the ligand points towards the Fe=O unit and show rather close C–H···O distances indicative of

Table 1: Selected bond lengths [Å] and Mössbauer parameters (mm s^{-1}) for **1**, **2**, and **3**.

	d(Fe–O)	d(Fe–C)	δ	ΔE_Q
1 (Fe^{II})	–	1.970(2)/1.986(2)/ 2.007(2)/2.022(2)	0.23	2.10
2 (Fe^{IV})	1.661(3)	1.979(5)/1.980(5)/ 2.037(5)/2.045(5)	−0.13	3.08
3 (Fe^{III})	1.752(2) 1.752(2)	1.970(4)/1.973(4)/ 2.028(4)/2.036(4)/ 1.947(4)/1.982(4)/ 2.012(4)/2.020(4)	0.04	2.56

weak hydrogen bonds (Figure 4, right). This situation is somewhat reminiscent of the trigonal bipyramidal complex reported by Borovik and co-workers, which has an Fe^{IV}=O unit within the cavity of three urea groups involved in N–H···O hydrogen bonds.[10] However, despite the C–H···O interactions in **2**, no decomposition products from ligand oxygenation have been observed (see below).

We were able to collect sufficient amounts of crystalline material of **2** to perform, for the first time for an oxoiron(IV) complex, a SQUID measurement. Magnetic susceptibility data were collected in the temperature range 2–200 K (to avoid decomposition at higher temperatures). No significant field dependence was observed when data were taken at applied fields of 0.2 and 0.5 T. The $\chi_M T$ value at 200 K of 0.98 $cm^3 K mol^{-1}$ (Figure 5, left) is close to the spin-only value

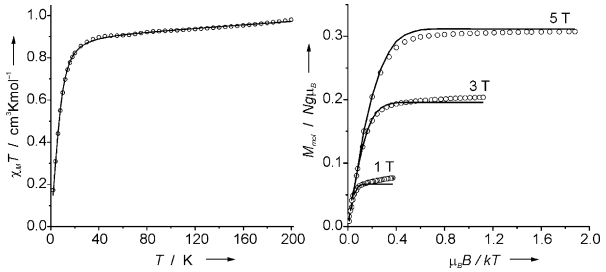

Figure 5. $\chi_M T$ versus T (left) and variable-temperature/variable-field (VTVH) magnetization measurements as M_{mol} versus B/T (right) for a crystalline sample of **2**.

for $S=1$ (1.00 $cm^3 K mol^{-1}$) and clearly shows the intermediate-spin state of the oxoiron(IV) unit in **2**. The decrease of the $\chi_M T$ curve below 40 K can be attributed to the effect of zero-field splitting. Indeed, analysis of the magnetic data according to the spin Hamiltonian that includes terms for zero-field and Zeeman splitting [Eq. (1)] leads to a good fit with values $g=1.89$ and $|D|=16.8\ cm^{-1}$.

$$\hat{H} = D(\hat{S}_z^2 - \frac{1}{3}S(S+1)) + g\mu_B \vec{B}\cdot\vec{S} \qquad (1)$$

Simulation of magnetization measurements at variable temperature and variable field (VTVH; Figure 5 right) gave $g=1.87$ and $D=+16.4\ cm^{-1}$; these values are in excellent agreement with those derived from susceptibility data and unambiguously confirm the positive sign of the zero-field splitting parameter. Though large, the anisotropy value of **2** is yet smaller than D for related oxoiron(IV) complexes based on non-heme[4] and porphyrin supporting ligands[22,24] (26–35 cm^{-1}), which likely originates from the large separation of the $S=1$ ground and $S=2$ excited states, and the relatively large splitting of the d_{xy} and d_{xz}/d_{yz} orbitals in the t_{2g} manifold of **2**.[25]

In MeCN, **2** was stable at −40 °C for more than one month. Upon warming, the solution became brown as a result of reduction of **2** to the binuclear μ-oxo diferric complex **3**, which was identified by ESI-MS ($[(L^{NHC})_2Fe_2O(OTf)_3]^+$: $m/z=1271.1$, calcd $m/z=1271.1$) and UV/Vis spectroscopy (characteristic band at 367 nm). Self-decay of a 0.12 mM MeCN solution of **2** was monitored by UV/Vis spectroscopy at room temperature (Figure 6); it exhibits a half-life of about five hours.[26] This decay rate is similar to the one reported for $[Fe^{IV}O(Bn\text{-}TPEN)]^{2+}$.[7] The time trace of the rising band at

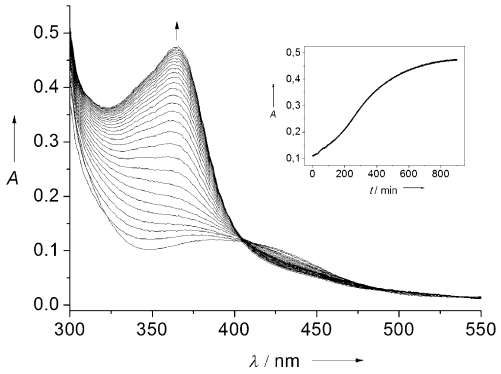

Figure 6. Self-decay of $[(L^{NHC})Fe^{IV}O(MeCN)](OTf)_2$ in MeCN at room temperature, monitored by UV/Vis spectroscopy. The inset shows the development of the 365 nm band, representing the formation of μ-oxo complex **3**.

365 nm suggests a more complicated mechanism; more detailed kinetic studies are underway. Complex **3** was also obtained by oxidation of **1** with *m*CPBA, trimethylamine N-oxide, or with aerial O_2 in MeCN. Surprisingly, in contrast to 2-(tBuSO$_2$)C_6H_4IO, reaction with parent iodosobenzene (C_6H_4IO) at −40 °C did not generate **2**, but gave **3** directly.

The molecular structure of **3** was determined by X-ray analysis of brown single crystals grown by slow diffusion of Et_2O into a MeCN solution (Figure 1, right). Both ferric ions are coordinated fivefold in square-pyramidal geometry. The oxygen atom is bound in an almost linear fashion with an Fe–O–Fe angle of 178.79(16)°. As expected, Fe–O distances are much longer (1.752(2) Å) than those in **2** because of decreased π-bonding, which is also reflected in slightly shorter Fe–C bonds (Table 1). SQUID data of **3** in the temperature range 2–295 K, simulated by using the Hamiltonian $\hat{H}=-2J\hat{S}_1\hat{S}_2$, showed an $S=0$ ground state and extremely strong antiferromagnetic coupling ($J=-606\ cm^{-1}$) of the two ferric ions (Figure S4). Unfortunately, however, the local spins could not be determined from the SQUID data because of the minute population of only the first excited state at 295 K; the data are consistent with iron spins $S_i=1/2$, 3/2, or 5/2. The coupling in any case appears to be the strongest reported for any μ-oxo diiron(III) complex investigated so far.[27] Effective diamagnetism of complex **3** was confirmed by sharp NMR signals.

Mössbauer spectra were collected for all three complexes **1**, **2**, and **3** at 80 K (solid samples for **1** and **3**; frozen solution in MeCN glass for **2**; Figure 7, top left). In the case of **2** and **3**, isomer shifts (δ) were found at rather low values (**2**: $-0.13\ mm\,s^{-1}$; **3**: $0.04\ mm\,s^{-1}$), and quadrupole splittings (ΔE_Q) were quite large (**2**: $3.08\ mm\,s^{-1}$; **3**: $2.56\ mm\,s^{-1}$; Table 1). A series of oxoiron(IV) complexes based on the tetramethylcyclam (TMC) ligand scaffold show isomer shifts within the narrow range 0.15–0.20 $mm\,s^{-1}$, much higher than for **2**. This result reflects the extremely strong equatorial σ-

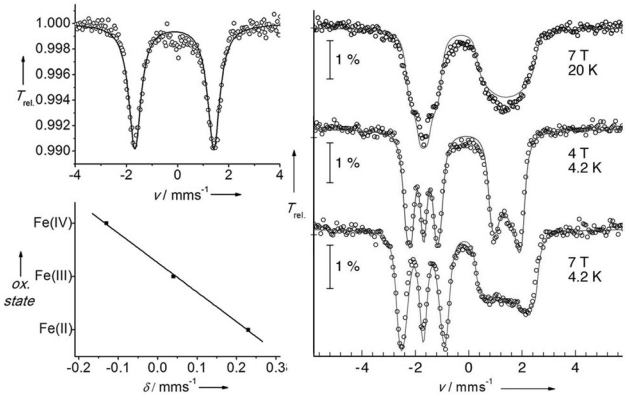

Figure 7. Top left: Mössbauer spectrum of $[(L^{NHC})Fe^{IV}O(MeCN)](OTf)_2$ (**2**) recorded at 80 K. Bottom left: Correlation of isomer shift versus oxidation state for complexes **1**, **2**, and **3**; linear fit is defined by: oxidation state = 3.3(1)–5.6(2) δ/mm s^{-1}. Right: Magnetic Mössbauer spectra of **2** (MeCN glass) recorded at 4.2 and 20 K with fields of 4 and 7 T applied perpendicular to the γ rays. The lines are the result of a spin Hamiltonian simulation for $S=1$ using fast spin relaxation with parameters given in the text.

donor strength of the macrocyclic tetracarbene ligand with pronounced charge donation into the iron 4 s orbital. Comparatively low isomer shifts have only been observed for an anionic Fe^{IV}=O complex with a tetraamido macrocyclic ligand, $[(TAML)Fe^{IV}O]^{2-}$ (-0.19 mm s^{-1}).[28,29] Similar arguments apply for **3**, because μ-oxo diferric complexes usually show isomer shifts in a range of 0.2–0.5 mm s^{-1}.[27] A plot of Mössbauer isomer shifts versus formal oxidation state for complexes **1**, **2**, and **3**, which all bear the same cyclic tetracarbene scaffold, shows an excellent linear correlation (oxidation state = 3.3(1)–5.6(2) δ/mm s^{-1}; Figure 7, bottom left). The slope is similar to that reported for a series of (cyclam)iron–oxo, (cyclam)iron–azido, and (cyclam)iron–nitrido complexes (oxidation state = 4.6(1)–5.0(3) δ/mm s^{-1}),[5] although in the present case, the function is shifted to lower δ values. In line with this result, ΔE_Q for **2** is much larger than for most other oxoiron(IV) complexes (typically in the range 0.16–1.39 mm s^{-1} for TMC-based systems).[3,4] This observation again reflects the oblate charge distribution around the iron nucleus in **2**, which arises from the large electronic charge donated by the equatorial tetracarbene into the $d_{x^2-y^2}$ orbital; the effect is almost as pronounced as in $[(TAML)Fe^{IV}O]^{2-}$ ($\Delta E_Q = 3.95$ mm s^{-1}).[28]

The magnetically split Mössbauer spectra for **2**, obtained at 4.2 and 20 K in fields of 4 and 7 T applied perpendicular to the γ beam (Figure 7, right), are consistent with the iron(IV) $S=1$ configuration. The spectra could be nicely simulated with spin-Hamiltonian parameters that are very similar to those obtained from magnetization measurements, rendering large, almost axial zero-field splitting ($D = 15 \pm 2$ cm^{-1}, g fixed at 2.0). Iterations of the rhombicity parameters showed a preference for weak distortion of the axial symmetry of the ligand field ($E/D = 0.08$), which is consistent with the less than fourfold rotation symmetry of the complex. A weak rhombicity is also reflected in the electric-field gradient ($\Delta E_Q = +3.09$ mm s^{-1}, $\eta = 0.3$), as well as in the magnetic hyperfine-coupling constants ($A/g_N\mu_N = [-17.1, -18.8, -2]$ T). The values, two large negative and one small negative,[3] resemble closely those of intermediate-spin oxoiron(IV) compounds with porphyrin ligands.[30]

The electronic structure of the iron(III) μ-oxo dimer (**3**) deserves particular attention, because according to our knowledge, iron(III) in this motif is usually considered to be high-spin.[27,31] In contrast, the low isomer shift in our case (0.04 mm s^{-1}) is clearly below the range of values ever observed for ferric high-spin iron. The values are diagnostic of low-spin, $S=1/2$, or also intermediate-spin $S=3/2$ iron(III);[22] the magnetic data unfortunately are not conclusive, as shown above. Although intermediate-spin might be possible because of the five coordination of the iron sites, we strongly favor the low-spin assignment, because the isomer shift fits perfectly into the correlation diagram of Figure 7. Such a straight correlation can hold only if the "titration" of valence electrons throughout the series of complexes **1** to **3** to **2** from ferrous via ferric to ferryl iron is restricted to either anti-bonding e_g orbitals or to non-bonding t_{2g} orbitals. Otherwise the expected irregular changes in bond lengths should induce irregular steps in the variation of the isomer shift.[22,32] Because **1** is a t_{2g}^6 and **2** a t_{2g}^4 compound, we conclude that **3** is t_{2g}^5, and thus represents a rare case of a low-spin iron(III) μ-oxo dimer.

In conclusion, we reported the first structurally characterized high-valent oxoiron(IV) complex that is not supported by an oligodentate N-donor ligand. Instead, the macrocyclic tetracarbene scaffold of **2** makes the key bioinorganic Fe^{IV}=O moiety applicable in organometallic chemistry. Complex **2** features high stability, which has enabled the first SQUID characterization of solid material of an oxoiron(IV) species, and thus provides additional information about its electronic structure. The strong in-plane σ-donating tetracarbene ligand efficiently stabilizes the intermediate-spin $S=1$ state over the $S=2$ state by raising the iron $d_{x^2-y^2}$ orbital. This situation gives rise to spectroscopic signatures of **2** that are quite unusual and reminiscent of the $[(TAML)Fe^{IV}O]^{2-}$ system, though the present $[(L^{NHC})Fe^{IV}O(RCN)]^{2+}$ is dicationic rather than dianionic. The macrocyclic tetracarbene also imparts unusual properties to the iron(III) μ-oxo dimer **3**, which appears to be a rare example of a low-spin species for this prominent motif. Studies directed toward the reactivity of the novel type of organometallic oxoiron(IV) complex and further elucidation of the electronic structures of **2** and **3** are in progress.

Received: October 5, 2012
Published online: November 28, 2012

Keywords: bioinorganic chemistry · mössbauer spectroscopy · N-heterocyclic carbene · organometallic chemistry · oxoiron(IV)

[1] a) C. Krebs, D. G. Fujimori, C. T. Walsh, J. M. Bollinger, *Acc. Chem. Res.* **2007**, *40*, 484–492; b) W. Nam, *Acc. Chem. Res.* **2007**, *40*, 522–531.

[2] a) M. Costas, M. P. Mehn, M. P. Jensen, L. Que, Jr., *Chem. Rev.* **2004**, *104*, 939–986; b) J. T. Groves, *J. Inorg. Biochem.* **2006**, *100*, 434–447.

[3] J. Hohenberger, K. Ray, K. Meyer, *Nat. Commun.* **2012**, *3*, 720 – 732.
[4] A. R. McDonald, L. Que, Jr., *Coord. Chem. Rev.* **2012**, DOI: 10.1016/j.ccr.2012.08.002.
[5] C. A. Grapperhaus, B. Mienert, E. Bill, T. Weyhermüller, K. Wieghardt, *Inorg. Chem.* **2000**, *39*, 5306 – 5317.
[6] J.-U. Rohde, J.-H. In, M. H. Lim, W. W. Brennessel, M. R. Bukowski, A. Stubna, E. Münck, W. Nam, L. Que, Jr., *Science* **2003**, *299*, 1037 – 1039.
[7] E. J. Klinker, J. Kaizer, W. W. Brennessel, N. L. Woodrum, C. J. Cramer, L. Que, Jr., *Angew. Chem.* **2005**, *117*, 3756 – 3760; *Angew. Chem. Int. Ed.* **2005**, *44*, 3690 – 3694.
[8] A. Thibon, J. England, M. Martinho, V. G. Young, Jr., J. R. Frisch, R. Guillot, J.-J. Girerd, E. Münck, L. Que, Jr., F. Banse, *Angew. Chem.* **2008**, *120*, 7172 – 7175; *Angew. Chem. Int. Ed.* **2008**, *47*, 7064 – 7067.
[9] J. England, Y. Guo, E. R. Farquhar, V. G. Young, Jr., E. Münck, L. Que, Jr., *J. Am. Chem. Soc.* **2010**, *132*, 8635 – 8644.
[10] D. C. Lacy, R. Gupta, K. L. Stone, J. Greaves, J. W. Ziller, M. P. Hendrich, A. S. Borovik, *J. Am. Chem. Soc.* **2010**, *132*, 12188 – 12190.
[11] S. Fukuzumi, Y. Morimoto, H. Kotanni, P. Naumov, Y.-M. Lee, W. Nam, *Nat. Chem.* **2010**, *2*, 756 – 759.
[12] K. Meyer, E. Bill, B. Mienert, T. Weyhermüller, K. Wieghardt, *J. Am. Chem. Soc.* **1999**, *121*, 4859 – 4876.
[13] J. F. Berry, E. Bill, E. Bothe, S. D. George, B. Mienert, F. Neese, K. Wieghardt, *Science* **2006**, *312*, 1937 – 1941.
[14] C. Vogel, F. W. Heinemann, J. Sutter, C. Anthon, K. Meyer, *Angew. Chem.* **2008**, *120*, 2721 – 2724; *Angew. Chem. Int. Ed.* **2008**, *47*, 2681 – 2684.
[15] J. J. Scepaniak, C. S. Vogel, M. M. Khusniyarov, F. W. Heinemann, K. Meyer, J. M. Smith, *Science* **2011**, *331*, 1049 – 1052.
[16] S. A. Cramer, D. M. Jenkins, *J. Am. Chem. Soc.* **2011**, *133*, 19342 – 19345.
[17] F. E. Hahn, V. Langenhahn, T. Lügger, T. Pape, D. L. Van, *Angew. Chem.* **2005**, *117*, 3825 – 3829; *Angew. Chem. Int. Ed.* **2005**, *44*, 3759 – 3763.
[18] H. M. Bass, S. A. Cramer, J. L. Price, D. M. Jenkins, *Organometallics* **2010**, *29*, 3235 – 3238.
[19] Very recently, a more convenient procedure for the synthesis of this type of tetracarbene complexes (92% yield for phenyl derivative of **1**) by transmetalation of silver carbenes has been published: Z. Lu, S. A. Cramer, D. M. Jenkins, *Chem. Sci.* **2012**, *3*, 3081 – 3087.
[20] S. Meyer, C. M. Orben, S. Demeshko, S. Dechert, F. Meyer, *Organometallics* **2011**, *30*, 6692 – 6702.
[21] N. Muresan, C. C. Lu, M. Ghosh, J. C. Peters, M. Abe, L. M. Henling, T. Weyhermüller, E. Bill, K. Wieghardt, *Inorg. Chem.* **2008**, *47*, 4579 – 4590.
[22] P. G. Debrunner in *Iron Porphyrins Part III*, *Vol. III* (Eds.: A. B. P. Lever, H. B. Gray), VCH, Weinheim, **1989**, p. 137.
[23] P. Gütlich, E. Bill, A. X. Trautwein, *Mössbauer Spectroscopy and Transition Metal Chemistry*, Springer, Berlin, **2011**, chap. 8.
[24] A. Gold, R. Weiss, *J. Porphyrins Phthalocyanines* **2000**, *4*, 344 – 349.
[25] F. Neese, *J. Inorg. Biochem.* **2006**, *100*, 716 – 726.
[26] At higher concentrations (0.60 and 3.0 mM), $\tau_{1/2}$ was found to be around three hours, however, because of the high concentrations, the decay of **2** could only be determined by the development of a band at 515 nm in these cases.
[27] D. M. Kurtz, Jr., *Chem. Rev.* **1990**, *90*, 585 – 606.
[28] A. Chanda, X. Shan, M. Chakrabarti, W. C. Ellis, D. L. Popescu, F. Tiago de Oliveria, D. Wang, L. Que, Jr., T. J. Collins, E. Münck, E. L. Bominaar, *Inorg. Chem.* **2008**, *47*, 3669 – 3678.
[29] Even a TMC-based oxoiron(V) complex appears to have a higher isomer shift of $+0.10\ \mathrm{mm\,s^{-1}}$: K. M. Van Heuvelen, A. T. Fiedler, X. Shan, R. F. De Hont, K. K. Meier, E. L. Bominaar, E. Münck, L. Que, Jr., *Proc. Natl. Acad. Sci. USA* **2012**, *109*, 11933 – 11938.
[30] a) C. E. Schulz, R. Rutter, J. T. Sage, P. G. Debrunner, L. P. Hager, *Biochemistry* **1984**, *23*, 4743 – 4754; b) R. Rutter, L. P. Hager, H. Dhonau, M. Hendrich, M. Valentine, P. Debrunner, *Biochemistry* **1984**, *23*, 6809 – 6816.
[31] Few low-spin iron(III) μ-oxo dimers have been reported: a) C. Ercolani, M. Gardini, K. S. Murray, G. Pennesi, G. Rossi, P. R. Zwack, *Inorg. Chem.* **1987**, *26*, 3539 – 3543; b) S. Sievertsen, K. S. Murray, B. Moubaraki, K. J. Berry, Y. Korbatieh, J. D. Cashion, L. J. Brown, H. Homborg, *Z. Anorg. Allg. Chem.* **1994**, *620*, 1203 – 1212; c) I. Vernik, D. V. Stynes, *Inorg. Chem.* **1996**, *35*, 2011 – 2018.
[32] F. Neese, *Inorg. Chim. Acta* **2002**, *337*, 181 – 192.

